J Neuropathol Exp Neurol
Vol. 68, No. 1
January 2009
pp. 48–58

ORIGINAL ARTICLE

Sirtuin 1 Reduction Parallels the Accumulation of Tau in Alzheimer Disease

Carl Julien, MSc, Cyntia Tremblay, MSc, Vincent Émond, PhD, Meryem Lebbadi, BSc, Norman Salem, Jr., PhD, David A. Bennett, MD, and Frédéric Calon, BPharm, PhD

Abstract

Aging and metabolism-related disorders are risk factors for Alzheimer disease (AD). Because sirtuins may increase the life span through regulation of cellular metabolism, we compared the concentration of sirtuin 1 (SIRT1) in the brains of AD patients (n = 19) and controls (n = 22) using Western immunoblots and in situ hybridization. We report a significant reduction of SIRT1 (messenger RNA [mRNA], −29%; protein, −45%) in the parietal cortex of AD patients, but not in the cerebellum. Further analyses in a second cohort of 36 subjects confirmed that cortical SIRT1 was decreased in AD but not in individuals with mild cognitive impairment. SIRT1 mRNA and its translated protein correlated negatively with the duration of symptoms (mRNA, $r^2 = -0.367$; protein, $r^2 = -0.326$) and the accumulation of paired helical filament tau (mRNA, $r^2 = -0.230$; protein, $r^2 = -0.119$), but weakly with insoluble amyloid-β 42 (mRNA, $r^2 = -0.090$; protein, $r^2 = -0.072$). A significant relationship between SIRT1 levels and global cognition scores proximate to death was also found ($r^2 = +0.09$, p = 0.049). In contrast, cortical SIRT1 levels remained unchanged in a triple-transgenic animal model of AD. Collectively, our results indicate that loss of SIRT1 is closely associated with the accumulation of amyloid-β and tau in the cerebral cortex of persons with AD.

From the Faculty of Pharmacy, Laval University (CJ, CT, VÉ, ML, FC); Molecular Endocrinology and Oncology Research Center, Centre Hospitalier de l'Université Laval Research Center (CJ, CT, VÉ, ML, FC), Quebec, Quebec, Canada; Section of Nutritional Neuroscience, Laboratory of Membrane Biochemistry and Biophysics, Division of Intramural Clinical and Biological Research, National Institute on Alcohol Abuse and Alcoholism, National Institutes of Health (NS), Rockville, Maryland; and Rush Alzheimer's Disease Center, Rush University Medical Center (DAB), Chicago, Illinois.

Send correspondence and reprint requests to: Frédéric Calon, BPharm, PhD, Molecular Endocrinology and Oncology Research Center, Centre Hospitalier de l'Université Laval Research Center, 2705 Laurier Blvd, Quebec, Quebec, Canada G1V 4G2; E-mail: frederic.calon@crchul.ulaval.ca

This work was supported by Grant MOP74443 from the Canadian Institutes of Health Research, by Grant ASC 0516 from the Alzheimer Society Canada, by Grant No. 10307 from the Canada Foundation for Innovation (to Frederic Calon), and by Grant No. P30AG10161 and R01AG15819 from the National Institute on Aging grants (to David Bennett). Carl Julien is supported by studentships from the Alzheimer Society Canada, Fonds de la Recherche en Santé du Québec, and Laval University "Fonds d'Enseignement et de Recherche." The work of Frédéric Calon was supported by a New Investigator Award from the Clinical Research Initiative and the CIHR Institute of Aging (CAN-76833).

Key Words: Sirtuins, Amyloid-β peptide, Cognitive function, Fatty acids, Mild cognitive impairment, Postmortem analysis, Silent information regulator 2 (Sir2).

INTRODUCTION

Alzheimer disease (AD) is a prevalent cause of the loss of cerebral functions and is mainly diagnosed postmortem by the accumulation of neurofibrillary tangles and amyloid-β (Aβ) plaques in the brain (1). Despite the identification of genetic and environmental factors, aging remains the main risk factor of AD. The incidence of AD is extremely low before the age of 65 years, and even in the presence of highly penetrant genetic factors, the development of AD is delayed until old age in most cases (2–4). In parallel, peripheral metabolic diseases, such as diabetes, obesity, and insulin resistance have been associated with an increased risk of developing AD (5–8). It is thus highly probable that molecular events linked with aging and metabolic processes are closely involved in AD pathogenesis.

Silent information regulator 2 (Sir2) proteins, or sirtuins (SIRTs), are protein deacetylases found in organisms ranging from bacteria to humans (9–11). Their nicotine adenine dinucleotide–dependent capacity to deacetylate both histone and nonhistone substrates is essential to the regulation of various cellular functions (9, 10). In mammals, SIRTs 1 to 7 have been identified as homologs of Sir2. From the 7 sirtuins in mammals, SIRT1 is the most closely related to Sir2 and has been the most studied (9, 10, 12, 13). In addition to histone targets, SIRT1 deacetylates various substrates including p53, forkhead transcription factor, nuclear factor-κB, and liver X receptor (12, 13). Most importantly, the capacity of SIRTs to promote longevity has been demonstrated in yeast, *Caenorhabditis elegans* and *Drosophila*, and is thought to act similarly in mammals (10, 14–18). Calorie restriction is one of the most consistent nongenetic strategies to prolong life span, whereas inducing SIRT activity (3, 9, 10, 13, 16) has been shown to reduce Aβ pathology and tau concentration, and improve cognitive performance in animal models of AD (19–22).

Because SIRT1 might regulate aging and metabolic processes involved in the pathogenesis of AD and could, therefore, represent a potential therapeutic target, the connection between SIRTs and AD has received much recent attention (9–11, 23). Specifically, SIRT1 has recently been shown to suppress γ-secretase activity in different in vitro models, thereby reducing the production of Aβ (24).

Reduction of γ-secretase activity has been replicated in vivo using transgenic mice that overexpress SIRT1, thus providing the first evidence linking calorie restriction, SIRTs, and AD (24). A correlative relationship between SIRT1 and Aβ load was also found in the brains of calorie-restricted nonhuman primates (21).

To investigate the regulation of SIRT1 and its link with the progression of AD, we compared SIRT1 protein and messenger RNA (mRNA) in postmortem brain samples from individuals with the neuropathologic diagnosis of AD with those from controls. SIRT1 was also studied in a second study cohort divided into 3 groups based on detailed antemortem assessment of cognitive function as no cognitive impairment (NCI), mild cognitive impairment (MCI), or AD. The relationships between brain SIRT1 protein and mRNA concentrations and all available neuropathologic, biochemical, and clinical indexes were investigated to identify significant correlations. At the current state of knowledge, such postmortem investigations are critical for determining the role of SIRTs as potential therapeutic targets in AD.

MATERIALS AND METHODS

Patients and Handling of Brain Tissue

Cohort No. 1: Douglas Hospital Research Center Brain Bank

Tissue from the parietal cortex, hippocampus, and cerebellum from 19 AD patients and 22 controls who died with no other neurological disorders were obtained from the Douglas Hospital Research Center Brain Bank (Montreal, Canada) and have been detailed elsewhere (25). All brain samples included in the present study were from patients from whom informed consent forms had been obtained from either the patient or a family member. Table 1 summarizes relevant information available for the subjects from Cohort No. 1. The diagnosis of AD was based on the neuropathologic examination as having "definite AD" or "probable AD" according to the Consortium to Establish a Registry for AD (CERAD 1–2) diagnostic criteria; controls were rated as "possible AD" or "no AD" (CERAD 3–4) (26).

Cohort No. 2: Religious Orders Study (Rush Alzheimer's Disease Center)

Samples from the parietal cortex from 36 individuals were divided into 3 groups based on clinical diagnoses (12 MCI, 12 AD, and 12 NCI), as described (27). The study volunteers were from the Religious Orders Study, a longitudinal clinicopathologic study of aging and dementia from which an extensive amount of clinical and neuropathologic data are available (28, 29). The institutional review board of Rush University Medical Center approved the study. Each participant underwent a uniform structured baseline clinical evaluation as described elsewhere (28–30). Briefly, the evaluation included a medical history, neurological examination, neuropsychological performance testing, review of a brain scan when available, and diagnostic classification by an examining physician. In addition to the Mini-Mental State

TABLE 1. Clinical and Biochemical Data of Cohort No. 1 From the Douglas Hospital Research Center Brain Bank

Clinical and Biochemical Data	Controls	AD	Statistical Analysis
n	22	19	
Men, %	55	47	C; Pearson test, $\chi^2 = 0.21$; p = 0.65
Age at first symptom, years	n/a	68.5 (9.0)	n/a
Duration of symptoms, years	n/a	7.7 (3.7)	n/a
Age at death, years	71.1 (9.1)	77.5 (8.8)*	Student *t*-test, p = 0.028
Postmortem delay, hours	18 (8)	18 (9)	Student *t*-test, p = 0.98
Brain mass, g	1,259 (134)	1,080 (141)†	Student *t*-test, p = 0.0002
Brain pH	6.16 (0.30)	6.22 (0.28)	Student *t*-test, p = 0.54
Total mRNA in cortex	3.0 (0.9)	3.1 (0.7)	Student *t*-test, p = 0.70
Total mRNA in cerebellum	4.7 (0.6)	4.5 (0.7)	Student *t*-test, p = 0.43
Soluble Aβ40 concentration	25 (22)	68 (55)‡	Student *t*-test, p = 0.0016
Insoluble Aβ40 concentration	21 (8)	125 (191)‡	Student *t*-test, p = 0.0142
Soluble Aβ42 concentration	240 (285)	782 (388)†	Student *t*-test, p < 0.0001
Insoluble Aβ42 concentration	626 (967)	2190 (1,521)†	Student *t*-test, p = 0.0003
Soluble total tau content	124 (26)	113 (26)	Student *t*-test, p = 0.21
Insoluble total tau content	404 (461)	9580 (5302)†	Student *t*-test, p < 0.0001
Total PHF_{tau} content	182 (159)	1736 (1689)†	Student *t*-test, p < 0.0001
Total n-3	3.0 (0.6)	2.8 (0.7)	Student *t*-test, p = 0.37
Total n-6	3.2 (0.8)	3.0 (0.7)	Student *t*-test, p = 0.27

Neuropathologic data were generated on coronal sections or immunoblots from the parietal cortex, and the diagnosis was based on CERAD neuropathologic criteria; brain pH was measured in cerebellum extracts. Values are expressed as means (SD) unless otherwise indicated.

Concentrations of Aβ are expressed in picograms per milligram of protein or nanograms per milligram of tissue in soluble and insoluble fractions, respectively. Tau content and levels of mRNA are expressed in relative optical density. Fatty acid composition is expressed in nanograms per gram of tissue. For more details on methodology, see Materials and Methods section and Julien et al (25).

*p < 0.05, †p < 0.001, ‡p < 0.01 versus CERAD 3 to 4 controls.

Aβ, amyloid-β peptide; AD, Alzheimer disease (CERAD 1–2); CERAD, Consortium to Establish a Registry for AD; C, Contingency; Controls; mRNA, messenger RNA; n-3, omega-3 polyunsaturated fatty acids; n-6, omega-6 polyunsaturated fatty acids; n/a, not applicable.

Examination, the 19 tests used in these analyses included measures of episodic memory, semantic memory, working memory, perceptual speed, and visuospatial ability (31). The composite measure of global cognition combined these 19 separate tests (31). At death, each case was assigned a Braak score based on neurofibrillary tau pathology, a senile plaque score based on modified CERAD criteria, and a diagnosis based on the National Institute on Aging–Reagan criteria by a neuropathologist blinded to all clinical data (30). Density of Aβ and paired helical filament tau (PHF_{tau}) staining area was determined in paraffin-embedded sections from the temporal cortex by immunohistochemistry using MO0872 and AT8 antibodies, respectively, as described (32). Neuritic plaques, diffuse plaques, and neurofibrillary tangles in the temporal cortex were counted after Bielschowsky silver staining, as previously described (33). Cerebellar pH was measured to assess the degree of preservation of the tissue (34, 35). Concentrations of Aβ and tau in the temporoparietal cortex were assessed using ELISA and Western immunoblotting, as described (27). Table 2 summarizes relevant data on Cohort No. 2 (27).

Tissue Handling

Tissue blocks were cut into coronal sections (20 μm) on a cryostat (−18°C) from which small punches (~50 mg) of tissue were extracted. Sections were used for in situ hybridization, whereas tissue extracts were kept for Western immunoblotting, ELISA, and/or gas chromatography (see later).

Animals

The triple transgenic model of AD (3×Tg-AD) was developed to produce age-dependent Aβ and tau pathology in the mouse brain (36). Male and female 3×Tg-AD mice were raised in our animal facilities with the approval of Laval University Animal Ethics Committee in accordance with the standards of the Canadian Council on Animal Care. Animals were perfused at different ages with 1× PBS containing a cocktail of protease inhibitors (SIGMAFAST Protease Inhibitor Tablets, Sigma-Aldrich, Oakbridge, Ontario, Canada) and phosphatase inhibitors (1 mmol/L each of sodium vanadate and sodium pyrophosphate, 50 mmol/L sodium fluoride). Brain regions were dissected from 1 hemisphere as previously described (37).

Sample Preparation

Tissue extracts were homogenized in 5 volumes of Tris buffered saline (TBS) containing a cocktail of protease inhibitors and phosphatase inhibitors as described (25). Samples were sonicated briefly (3 × 10 seconds) and

TABLE 2. Clinical and Biochemical Data of Subjects From Cohort No. 2 (Religious Order Study)

Characteristics	NCI	MCI	AD	Statistical Analysis
n	12	12	12	
Men, %	8.4	50	25	C; Pearson test, $\chi^2 = 5.26$; $p = 0.07$
Mean education, years	17.5 (3.9)	19.6 (2.4)	18.0 (2.8)	A; $F_{2,33}$ (groups) = 1.49; $p = 0.24$
Mean MMSE	27.4 (2.0)	26.9 (2.2)	16.2 (8.9)*	A; $F_{2,33}$ (group) = 16.57; $p < 0.0001$
Global cognition score	−0.12 (0.23)	−0.43 (0.46)	−1.75 (0.96)*	A; $F_{2,32}$ (group) = 22.22; $p < 0.0001$
ApoE ε4 allele carriage, %	25	33	50	C; Pearson test, $\chi^2 = 1.69$; $p = 0.43$
Age at death, years	85.0 (6.0)	84.5 (3.8)	86.1 (5.8)	A; $F_{2,33}$ (groups) = 0.29; $p = 0.75$
Postmortem delay, days	7.4 (6.4)	6.0 (4.1)	6.3 (3.9)	A; $F_{2,33}$ (groups) = 0.26; $p = 0.77$
Cerebellar pH	6.36 (0.31)	6.46 (0.21)	6.49 (0.37)	A; $F_{2,33}$ (groups) = 0.62; $p = 0.55$
Aβ IHC density	0.9 (1.2)	1.8 (1.7)	4.7 (3.0)†	A; $F_{2,22}$ (group) = 7.66; $p = 0.003$
PHF_{tau} IHC density	1.0 (2.6)	4.0 (7.3)	26.8 (35.5)‡	A; $F_{2,27}$ (group) = 4.59; $p = 0.019$
Neuron plaque counts	2.3 (2.8)	4.7 (4.3)	25.9 (26.5)§	A; $F_{2,33}$ (group) = 8.12; $p = 0.0014$
Neuron diffuse plaque counts	12.3 (23.8)	22.8 (26.2)	20.4 (17.2)	A; $F_{2,33}$ (groups) = 0.69; $p = 0.51$
Soluble Aβ40 concentration	0.7 (1.0)	0.3 (0.6)	0.5 (0.6)	A; $F_{2,33}$ (groups) = 0.90; $p = 0.42$
Insoluble Aβ40 concentration	1.9 (4.0)	0.2 (0.6)	20.42 (17.22)	A; $F_{2,33}$ (groups) = 1.24; $p = 0.30$
Soluble Aβ42 concentration	4.5 (4.5)	5.9 (7.0)	0.8 (2.3)	A; $F_{2,33}$ (groups) = 1.93; $p = 0.16$
Insoluble Aβ42 concentration	1.0 (1.0)	1.1 (1.3)	2.5 (1.6)‖	A; $F_{2,33}$ (groups) = 4.65; $p = 0.015$
Soluble total tau content	1.0 (0.2)	1.1 (0.2)	0.9 (0.2)	A; $F_{2,33}$ (groups) = 2.51; $p = 0.10$
Insoluble total tau content	0.6 (0.2)	0.9 (0.7)	1.5 (0.9)†	A; $F_{2,33}$ (groups) = 5.46; $p = 0.009$
Total PHF_{tau} content	3.7 (2.8)	8.8 (13.0)	29.1 (37.2)‡	A; $F_{2,33}$ (groups) = 4.16; $p = 0.024$
CERAD score 4/3/2/1 (n)	3/3/5/1	6/0/4/2	0/1/3/8	n/a
Braak Score I/II/III/IV/V (n)	2/0/6/4/0	0/0/5/6/1	0/0/5/1/6	n/a
Reagan score 3/2/1 (n)	7/5/0	6/5/1	1/5/6	n/a

Neuropathologic data were generated from tissue sections and immunoblots from the temporal and/or parietal cortex; diagnoses were based on clinical evaluation; brain pH was measured in cerebellar extracts. Values are expressed as means (SD) unless otherwise indicated.

Aβ concentrations are expressed in picograms per milligram of protein or nanograms per milligram of tissue in soluble and insoluble fractions, respectively. Tau content is expressed in relative optical density from immunoblots. See Materials and Methods section and Tremblay et al (27).

Intergroup comparisons: *$p < 0.001$ versus NCI and MCI, †$p < 0.01$ versus NCI and $p < 0.05$ versus MCI, ‡$p < 0.05$ versus NCI, §$p < 0.01$ versus NCI or MCI, ‖$p < 0.05$ versus NCI or MCI.

A, ANOVA; Aβ, amyloid-β peptide; ApoE, apolipoprotein E; C, Contingency; CERAD, Consortium to Establish a Registry for AD; IHC, immunohistochemistry; MCI, mild cognitive impairment; MMSE, Mini-Mental State Examination; n/a, not applicable; NCI, no cognitive impairment; PHF_{tau}, paired helical filament tau.

centrifuged at 100,000 × *g* for 20 minutes at 4°C to generate a TBS-soluble fraction containing intracellular and extracellular proteins (TBS-soluble fraction). The TBS-insoluble pellet was sonicated in 5 volumes of lysis buffer (150 mmol/L NaCl, 10 mmol/L NaH_2PO_4, 1% Triton X-100, 0.5% sodium dodecyl sulfate, and 0.5% deoxycholate) containing the same protease and phosphatase inhibitor cocktail. The resulting homogenate was centrifuged at 100,000 × *g* for 20 minutes at 4°C to produce a lysis buffer-soluble fraction (detergent-soluble fraction). The pellets were homogenized in 5 volumes of 99% formic acid followed by a short sonication (3 × 10 seconds). The resultant suspension was centrifuged (100,000 × *g*, 4°C, 20 minutes) to generate a formic acid extract (detergent-insoluble fraction). Fifty microliters of this supernatant were neutralized with a 1:30 dilution of Tris-base 1 mol/L (pH 10) to be used for ELISA. The rest of the supernatant was dried by SpeedVac (Thermo Savant, Waltham, MA), solubilized in Laemmli buffer and processed for Western immunoblotting.

ELISA

Concentrations of Aβ40 and Aβ42 in the brain parietal cortex were measured with the Aβ40/β42 ELISA (HS) kits (The Genetics Company, Schlieren, Switzerland), as described (25, 27).

Western Immunoblotting

The protein concentration in each fraction was determined using bicinchoninic acid assays (Pierce, Rockford, IL). Equal amounts of protein per sample (15 mg of total protein per lane) were added to Laemmli loading buffer, heated to 95°C for 5 minutes before loading, and subjected to sodium dodecyl sulfate–polyacrylamide gel electrophoresis. Proteins were electroblotted onto polyvinylidene difluoride membranes (Immobilon, Millipore, MA) before blocking in 10% nonfat dry milk and 0.1% gelatin in PBS for 1 hour. Membranes were immunoblotted with appropriate primary and secondary antibodies followed by chemiluminescence reagents (ECL, Amersham/Pharmacia Biotech, Piscataway, NJ, or Supersignal from Pierce). Band intensities were quantified using a KODAK Image Station 4000 Digital Imaging System (Molecular Imaging Software version 4.0.5f7, KODAK, New Haven, CT). The following primary antibodies were used in this study: drebrin (clone M2F6; MBL, Woburn, MA), p21-activated kinase (PAK1/2/3; Cell Signaling Technology, Danvers, MA), ROCK1 (Chemicon, Temecula, CA), SIRT1 (anti-Sir2; Upstate, Chicago, IL), SNAP-25 (clone SMI 81; Covance, Berkeley, CA), synaptophysin (clone SVP-38; Chemicon), total tau (tau-13, Covance), anti-PHF_{tau} (AD2, Bio-Rad, Hercules, CA), and actin (Chemicon).

In Situ Hybridization

In situ hybridization procedures were performed essentially as described (25), at room temperature unless otherwise noted. Oligonucleotide sequences used correspond to bases 461-420 (h461: CGCCGCCTCTTCCTCCTCCTC GCCCTCGTCGTCGTCGTCTTC) and 328-289 (h328: GCCTCTTGCTCCCCGCCTGCCGCCGCCGCCTCTGCC TCCG) of human SIRT1 mRNA (NM_012238) (38). The series of in situ hybridization experiments were performed in parallel; total mRNA level was assessed with a 35-mer T-only probe targeting poly-A tails. Oligonucleotides were labeled with ^{33}P-dATP (PerkinElmer, Wellesley, MA) using a 3-terminal deoxynucleotidyltransferase enzyme kit (GE Healthcare, Baie d'Urfé, Quebec, Canada). The reaction was carried out at 37°C for 60 minutes, and labeled oligonucleotides were purified using a QIAquick Nucleotide Removal Kit (Qiagen, Mississauga, Ontario, Canada). The purified probes were kept at −20°C until the assay on the next day.

Tissue sections were dried under vacuum with desiccant at 4°C, were fixed for 5 minutes in 4% paraformaldehyde (Electron Microscopy Sciences, Hatfield, PA) in 0.1 mol/L of sodium phosphate buffer (PBS; pH 7.4), and then rinsed twice for 5 minutes each in PBS. The sections were then incubated in a fresh solution of 0.25% acetic anhydride in 0.1 mol/L of triethanolamine (pH 8.0) for 10 minutes. They were then rinsed (2 minutes) twice in 2× standard saline citrate (SSC; 1× SSC is 0.15 mol/L of NaCl, 0.015 mol/L of trisodium citrate, pH 7.0) and dehydrated through a series of ascending concentrations of ethanol (70%, 85%, and 95%, 1 minute each), air-dried, and stored 2 to 3 hours under vacuum with desiccant.

The 2 SIRT1 oligonucleotide probes (h461:h328, ratio 2:1) were diluted (10,000 c.p.m./mL final) in the hybridization buffer containing 50% deionized formamide, 10% dextran sulfate, 1× Denhardt solution, 0.25 mg/mL yeast tRNA, 0.5 mg/mL denatured salmon sperm DNA, and 4× SSC. Hybridization was performed at 37°C for 18 hours in a humid chamber with each slide covered with a glass coverslip. Sections were then washed successively in 2× SSC (90 minutes), 1× SSC (120 minutes), 0.5× SSC (30 minutes, 42°C), 0.5× SSC (30 minutes), 0.5× SSC (30 minutes, 50°C). Finally, the slides were dehydrated in a series of ascending concentrations of ethanol (70%, 85%, and 95%, 1 minute each), air-dried, and exposed to Kodak Biomax MR film for 28 days. Unless specified otherwise, hybridization products were obtained from Sigma-Aldrich (Oakbridge, Ontario, Canada).

Optical densities within subregions were macroscopically quantified on the KODAK IS 4000MM Digital Imaging System. Computed optical density data corresponded to the mean of all pixels inside the delimited areas of the parietal cortex, dentate gyrus/CA1/CA3 regions of the hippocampus, or the cerebellum. The hybridization signal value from a single section was obtained after subtracting the labeling from the white matter quantified in the same section. The final data from each individual was from the mean of 4 to 8 tissue sections. Nonspecific hybridization to tissue sections was found to be negligible, as determined by adding a 100-fold excess of unlabeled probes. To control for total mRNA content, we measured poly-A mRNA expression, and this did not differ between experimental groups (Table 1).

Gas Chromatography

Fatty acid profiles of samples from Cohort No. 1 were generated using gas chromatography and flame ionization

detection, using a previously reported methodology (39, 40). Approximately 30 mg of frozen cortical tissue from each sample was used for the present study. Weighed brain tissues were homogenized with BHT-Methanol (Sigma, St Louis, MO) and with 22:3n-3 methyl ester internal standard (NuChek Prep company, Elysian, MN) at a concentration of 500 μg/g of tissue. Extraction of lipids and transmethylation was performed as described (41), and fatty acid methyl esters were quantified on a model 6890 series gas chromatograph (Agilent Technologies, Palo Alto, CA) using a FAST-GC method (39, 40).

Data and Statistical Analyses

Statistical comparisons of data between AD patients and controls were performed using the Student *t*-test for unpaired values when appropriate. Statistical comparisons of means between more than 2 groups were performed using an analysis of variance (ANOVA) followed by Tukey-Kramer post hoc tests. When homogeneity of variance was not confirmed ($p > 0.05$ using Bartlett test), Welch ANOVA followed by Dunnett post hoc tests were computed. In addition, variances were reduced using logarithmic transformations to provide more normally distributed measures when needed. Coefficients of correlation and significance of the degree of linear relationship between parameters were determined with a simple regression model, and all statistical analyses were done using JMP Statistical Analysis Software (version 5.0.1).

RESULTS

Comparison Between Subjects

Table 1 shows that AD patients (CERAD 1–2) and controls (CERAD 3–4) from Cohort No. 1 (Douglas Hospital Research Center Brain Bank) were comparable with respect to sex, postmortem delay, cerebellar pH, and total poly-A mRNA content in gray matter from the brain cortex or cerebellum. Controls were significantly younger (−6.4 years; $p = 0.0283$) than subjects with AD (Table 1). Massive increases in Aβ40, Aβ42, and total tau were measured in fractions containing soluble (i.e. TBS) and insoluble (formic acid extracts) proteins (Table 1). Similarly, PHF_{tau} was increased by 867% in formic acid extracts of parietal cortex homogenates (Table 1). No significant changes in brain fatty acid profiles were detected between the 2 groups of persons (Table 1 and data not shown). Alzheimer disease biochemical data have been presented in detail elsewhere (25).

Table 2 summarizes clinical, neuropathologic, and biochemical data from Cohort No. 2 (Religious Orders Study) as grouped by clinical diagnoses. Individuals with AD showed a significant cognitive deficit as assessed with Mini-Mental State Examination and global cognition measures compared with persons with MCI and NCI (Table 2). Accumulation of tau PHF_{tau} and Aβ42 in the cerebral cortex was more prominent in AD, as demonstrated with immunostaining (Aβ or PHF_{tau} density), Bielschowsky silver impregnation (plaque counts), ELISA (Aβ concentration), and Western immunoblotting (tau levels) (Table 2). Complete information on these patients was previously published (27).

Lower SIRT1 Levels in AD Patients From Cohort No. 1

Representative examples of SIRT1 immunostaining as seen on Western immunoblot of TBS-soluble fractions are shown in Figure 1A. Two bands immunoreactive to SIRT1 were detected at approximately 110 kDa, consistent with reports also showing the presence of a SIRT1 doublet in murine and human cells (15, 42). The predicted molecular weight of SIRT1 is 82 kd; posttranslational events such as glycosylation, phosphorylation, or ubiquitination might explain differences in gel migration leading to the detection of 2 SIRT1 bands around 110 kd.

Western immunoblot analysis of samples from Cohort No. 1 revealed lower SIRT1/actin ratios in the parietal cortex (−45%; $p = 0.0087$, unpaired Student *t*-test) of AD patients (CERAD 1 or 2) compared with controls (CERAD 3 or 4; Fig. 1B). No differences were observed in hippocampal or cerebellar samples (Fig. 1B). Because SIRT1 showed no trend for correlation with the age of death ($r^2 = 0.03$, $p = 0.332$; Table 3), differences in SIRT1/actin ratio cannot be explained by the younger ages of the controls compared with the AD patients.

To determine whether the alteration in SIRT1 was present at the level of transcription, we performed in situ hybridization in the same series of samples. Figure 2A shows representative examples of the in situ hybridization of SIRT1 mRNA on parietal cortex, hippocampal, and cerebellar sections. Addition of unlabeled oligonucleotides (100×)

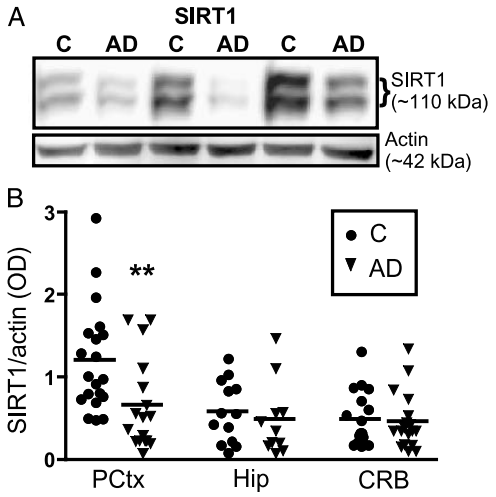

FIGURE 1. Lower sirtuin 1 (SIRT1) protein concentration in the cerebral cortex of patients with advanced Alzheimer disease (AD). **(A)** Representative immunoblots from homogenates of the parietal cortex of control subjects and AD patients. **(B)** Sirtuin 1 concentrations normalized to actin in homogenates from the parietal cortex, the hippocampus and the cerebellum from control subjects (Consortium to Establish a Registry for AD [CERAD] 3–4) and persons diagnosed with AD (CERAD 1–2) based on CERAD neuropathology stages. Values are expressed as SIRT1/actin ratios based on relative optical densities (each point represents an individual and the horizontal bar is the average). **$p < 0.01$ versus control subjects. C, controls; CRB, cerebellum; Hip, hippocampus; kd, kilodaltons; OD, relative optical density; PCtx, parietal cortex.

completely abolished the signal from the specific hybridization; the 2 oligonucleotide probes tested led to an identical signal distribution, consistent with their specificity for SIRT1 mRNA (not shown).

SIRT1 mRNA levels in the parietal cortex of individuals diagnosed as definite or probable AD based on CERAD stages were significantly lower than levels in the controls (−29%, p = 0.0055, unpaired Student *t*-test; Fig. 2B). In

TABLE 3. Clinical and Biochemical Correlates of SIRT1 Loss

	SIRT1 mRNA		SIRT1	
Markers	**n**	r^2	**n**	r^2
Duration of symptoms, years				
All subjects	16	−0.367*	16	−0.326*
Controls	—	—	—	—
AD	16	−0.367*	16	−0.326*
Brain weights, g				
All subjects	41	+0.173†	37	+0.159*
Controls	22	n.s.	20	n.s.
AD	19	n.s.	17	n.s.
Age at death, years				
All subjects	41	n.s.	37	n.s.
Controls	22	n.s.	20	n.s.
AD	19	n.s.	17	n.s.
Soluble Aβ42				
All subjects	40	−0.104*	37	n.s.
Controls	21	n.s.	20	n.s.
AD	19	n.s.	17	n.s.
Insoluble Aβ42				
All subjects	41	n.s.	72	−0.072*
Controls	22	n.s.	33	n.s.
AD	19	n.s.	39	n.s.
Insoluble/soluble tau ratio				
All subjects	39	−0.161*	36	−0.176*
Controls	20	n.s.	19	n.s.
AD	19	n.s.	17	n.s.
PHF_{tau}				
All subjects	41	−0.230†	72	−0.119†
Controls	22	n.s.	33	n.s.
AD	19	n.s.	39	−0.110*
EPA				
All subjects	41	n.s.	37	n.s.
Controls	22	n.s.	20	n.s.
AD	19	n.s.	17	−0.254*
DHA				
All subjects	41	n.s.	37	n.s.
Controls	22	n.s.	20	n.s.
AD	19	n.s.	17	+0.315*

Diagnoses were based on CERAD neuropathologic criteria (controls, CERAD 3–4; AD patients, CERAD 1–2). SIRT1 protein values used for correlative analyses were normalized to actin. Soluble and insoluble Aβ values were expressed as femtograms per microgram of protein and as picograms per milligram of tissue, respectively. The EPA and DHA values were expressed as nanograms per gram of tissue. The PHFtau was measured with the AD2 antibody.

*p < 0.05, †p < 0.01.

(−), Negative correlation; (+), positive correlation; Aβ, amyloid-β peptide; AD, Alzheimer disease patients; All, all subjects; C, controls; CERAD, Consortium to Establish a Registry for AD; DHA, docosahexaenoic acid; EPA, eicosapentaenoic acid; mRNA, messenger RNA; n.s., not significant; PHFtau, paired helical filament tau; SIRT1, sirtuin 1.

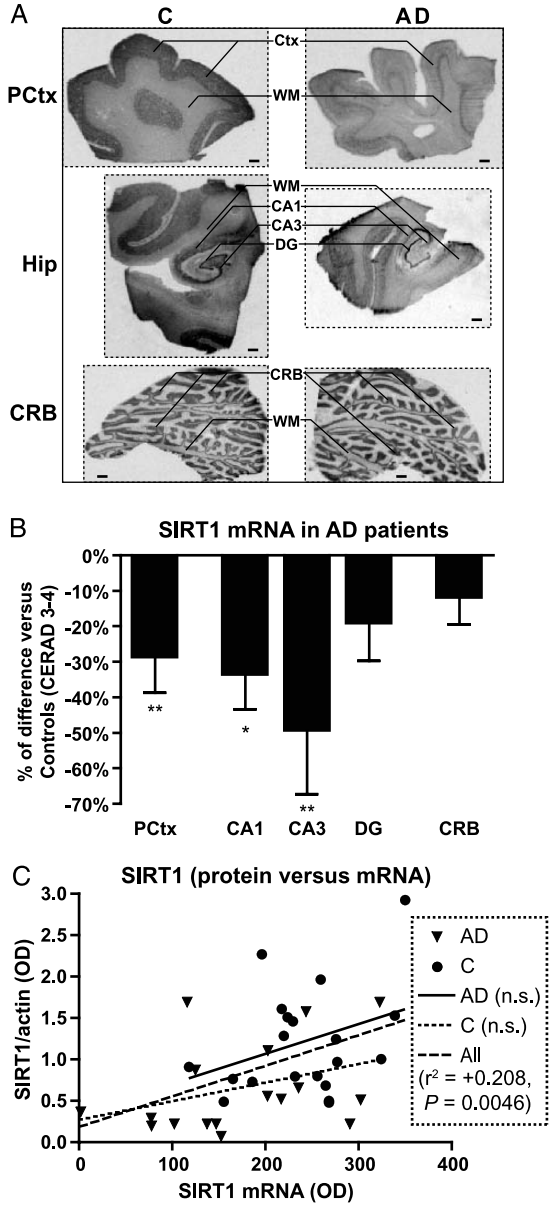

FIGURE 2. Lower sirtuin 1 (SIRT1) messenger RNA (mRNA) levels in the brain cortex and hippocampus of patients with advanced Alzheimer disease (AD). **(A)** Representative autoradiograms of parietal cortex (PCtx), hippocampus (Hip), and cerebellum (CRB) showing hybridization of [^{33}P]-labeled probes to SIRT1 mRNA in a control (C) and an AD patient (Scale bar = 2 mm). **(B)** Quantification of SIRT1 mRNA expression in the PCtx, CA1, CA3, and dentate gyrus (DG) region of the Hip and in the CRB. **(C)** Correlation between SIRT1 mRNA content and SIRT1 protein levels. Values are expressed as percentage (mean ± SEM) of relative optical density (OD) compared with Consortium to Establish a Registry for AD (CERAD) 3 to 4 controls. Diagnoses were based on CERAD criteria (controls, CERAD 3–4; AD patients, CERAD 1–2). *p < 0.05, **p < 0.01 versus control levels. CA1 and CA3, CA1 and CA3 areas of the hippocampus; n.s., not significant; WM, white matter.

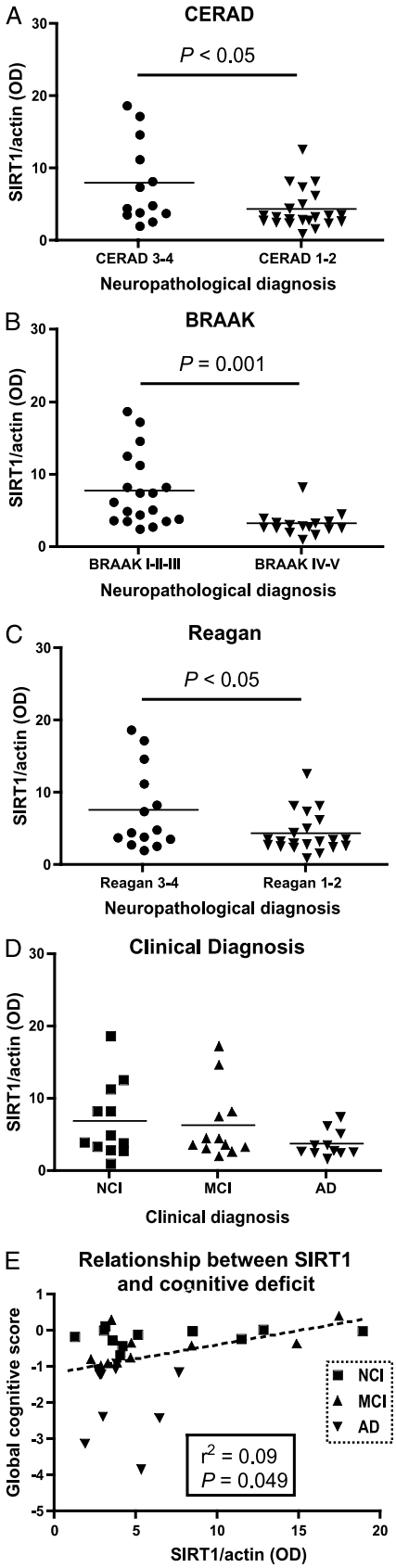

contrast to the protein data, there were also differences in SIRT1 mRNA in the CA1 (−34%, p = 0.0128) and CA3 (−49%, p = 0.0053) regions of the hippocampus of AD patients compared with those of the controls, but there were no differences in the dentate gyrus or cerebellar samples (Fig. 2B). The age at death was not associated with SIRT1 mRNA level in the parietal cortex (r^2 = 0.034, p = 0.249; Table 3). Sirtuin 1 mRNA content correlated positively with SIRT1 protein levels in the cerebral cortex (r^2 = +0.208, p = 0.0046; Fig. 2C), but not in the cerebellar cortex (r^2 = 0.05, p = 0.175; not shown).

Lower SIRT1 Levels Were Not Observed in MCI Subjects From Cohort No. 2

To determine whether the lower SIRT1 was related to the diagnosis of AD based on either the neuropathology or the clinical evaluation, we performed immunoblotting in a second cohort of participants with extensive antemortem clinical information from the Religious Orders Study. We again found a lower SIRT1 in individuals in whom the diagnosis of AD was supported by CERAD, Braak, and Reagan neuropathologic rating scales (Figs. 3A–C; unpaired Student *t*-test, unequal variance). Sirtuin 1 levels were, however, only moderately different between groups when the cases were divided according to the clinical diagnosis; these differences were not significant (Fig. 3D; Welch ANOVA, $F_{2,18}$ (groups) = 2.84; p = 0.085). It is noteworthy that SIRT1 concentrations were very similar between individuals with MCI and noncognitively impaired subjects (Fig. 3D).

SIRT1 Correlated With Markers of Disease Severity

As shown in Figure 3E, the levels of SIRT1 in the temporoparietal cortex normalized to actin showed a weak but significant linear relationship with antemortem composite indices of global cognition (r^2 = +0.09, p = 0.049). More detailed analyses revealed that SIRT1 also correlated linearly with episodic memory (r^2 = + 0.09, p = 0.043) and perceptual speed (r^2 = + 0.10, p = 0.037) but not with semantic memory (r^2 = 0.04, p = 0.130), working memory (r^2 = 0.02, p = 0.204), or visuospatial ability (r^2 = 0.02, p = 0.202; data not shown). We next examined the relationship between the levels of SIRT1, markers of AD neuropathology, and clinical

FIGURE 3. Relationship between postmortem cortical sirtuin 1 (SIRT1) concentration, neuropathologic diagnoses, clinical diagnosis, and global cognition score. Severe Alzheimer disease (AD) neuropathology as assessed by **(A)** Consortium to Establish a Registry for AD (CERAD), **(B)** Braak, and **(C)** National Institute on Aging–Reagan criteria was associated with lower SIRT1 protein levels. **(D)** Cortical SIRT1 content was not significantly different among individuals with no cognitive impairment (NCI), mild cognitive impairment (MCI), or AD, based on the clinical evaluation (Welch analysis of variance). **(E)** There is a significant relationship between SIRT1 and the antemortem global cognition score. Values are expressed as SIRT1/actin ratios based on relative optical densities (each point represents an individual; horizontal bars indicate averages).

or biochemical variables by performing a series of correlative analyses. We found strong significant inverse correlations between SIRT1 and the time between the initial diagnosis and death ("duration of symptoms," Table 3). A significant positive relationship between SIRT1 and brain weight was also observed (Table 3). On the other hand, no significant association between SIRT1 and the age at death was seen in any group (Table 3).

Interestingly, the levels of SIRT1 were inversely correlated with insoluble AD2-stained hyperphosphorylated paired helical filament tau (Table 3) and total insoluble tau (not shown). Sirtuin 1 loss was also associated with the conversion from normal soluble tau into insoluble tau (insoluble/soluble total tau ratio) (Table 3). Overall, the relationship between SIRT1 and accumulation of Aβ was weaker than with markers of tau pathology. Nevertheless, inverse correlations were detected between SIRT1 mRNA and soluble Aβ40 (not shown), and soluble Aβ42 (Table 3), whereas SIRT1 correlated negatively with insoluble Aβ42 (Table 3), but not with insoluble Aβ40, age, postmortem delay, or brain pH (Table 3 and data not shown). Because Rho-associated coiled-coil protein kinase 1 (ROCK1) is a possible mediator of the effect of SIRT1 on Aβ production (21, 24), we also measured ROCK1 in the parietal cortex of our 2 cohorts using Western immunoblots, but no significant change was observed (not shown).

Because AD is also characterized by a loss of synaptic proteins drebrin, synaptophysin, and PAK (37, 43, 44), we assessed the relationship between SIRT1 and selected synaptic markers. We observed that the SIRT1 decrease correlated with reduction of PAK and SNAP-25, particularly within subjects with a CERAD-based AD diagnosis (Table 4).

TABLE 4. Correlations Between SIRT1 and SIRT1 mRNA and Synaptic Proteins

		SIRT1 mRNA	SIRT1
Markers	**n**	r^2	r^2
Drebrin			
All subjects	37–41	n.s.	n.s.
Controls	20–22	n.s.	n.s.
AD	17–19	n.s.	n.s.
SNAP-25			
All subjects	37–41	n.s.	n.s.
Controls	20–22	n.s.	n.s.
AD	17–19	0.208* (+)	n.s.
Synaptophysin			
All subjects	37–41	n.s.	n.s.
Controls	20–22	n.s.	n.s.
AD	17–19	n.s.	n.s.
PAKs			
All subjects	37	0.237† (+)	0.378† (+)
Controls	20–21	n.s.	0.208* (+)
AD	17–19	0.268* (+)	0.451‡ (+)

Diagnoses were based on CERAD neuropathologic criteria (controls, CERAD 3–4; AD patients, CERAD 1–2). All protein values used for correlative analyses were normalized to actin, except when performed on the same gel.

*$p < 0.05$, †$p < 0.001$, ‡$p < 0.01$.

(−), Negative correlation; (+), positive correlation, AD, Alzheimer disease; CERAD, Consortium to Establish a Registry for AD; mRNA, messenger RNA; n.s., not significant; PAKs, p21-activated kinases; SIRT1, sirtuin 1; SNAP-25, synaptosome-associated protein-25.

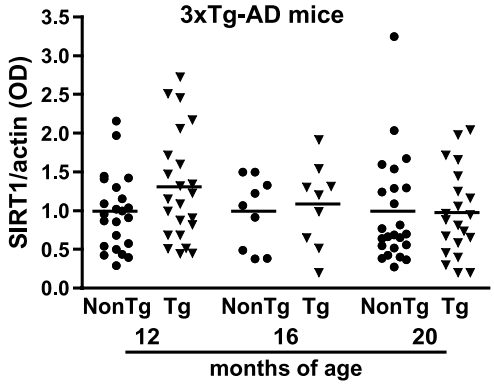

FIGURE 4. Sirtuin 1 (SIRT1) protein levels are constant in 12-, 16-, and 20 month-old triple transgenic model of AD (3×Tg-AD or Tg) and control nontransgenic littermate (NonTg) mice. Values are expressed as SIRT1/actin ratios based on relative optical densities ([ODs] each point represents a single mouse; horizontal bars indicate averages).

SIRT1 Correlated With Docosahexaenoic Acid Concentration

Epidemiological analyses and studies in animal models suggest that a deficiency in omega-3 polyunsaturated fatty acid (n-3 PUFA) intake plays a role in the development of AD (37, 45–48). Because of the role of SIRTs in various metabolic and cellular pathways, it has been recently hypothesized that n-3 PUFA effect is related to regulation of SIRT1 expression (49). Therefore, concentrations of fatty acids in brain tissue were determined using gas chromatography and studied in relation to SIRT1 levels. Our analysis did not reveal a significant difference in the concentrations of the 2 major n-3 PUFA, docosahexaenoic (DHA; 22:6n-3) and eicosapentaenoic acid (EPA; 20:5n-3), between samples from controls and AD patients (not shown). On the other hand, a positive relationship between SIRT1 protein and DHA concentration was significant in AD subjects ($r^2 = +0.315$, $p = 0.0190$; Table 3). Intriguingly, we detected an inverse relationship between SIRT1 and EPA ($r^2 = -0.254$, $p = 0.0394$), the main precursor of DHA in the brain from the same patients (Table 3).

SIRT1 Did Not Differ in 3×Tg-AD Mice at 12, 16, and 20 Months of Age

The triple-transgenic mouse model of AD (3×Tg-AD) developed by LaFerla and colleagues displays evidence of both Aβ and tau pathologies in AD-relevant brain regions (36). Antibody-based assessments indicate that both Aβ plaques and tau-loaded neurofibrillary tangles are readily detected in the 3×Tg-AD mice at 12 months of age and continue to accumulate thereafter (36, 50, 51). To determine whether overproduction of pathogenic mutant Aβ and tau directly alters brain SIRT1 concentrations, we performed Western immunoblotting on homogenates from the parietal

cortex of 3×Tg-AD mice. Very similar levels of SIRT1 were found in the cortex of 12-, 16-, and 20-month-old 3×Tg-AD mice compared with control nontransgenic littermates (Fig. 4), indicating that this model does not reproduce the SIRT1 loss found in AD brains.

DISCUSSION

To our knowledge, this study provides the first direct evidence for downregulation of SIRT1 in AD. Quantitative assessment of SIRT1 expression established a relationship between SIRT1, AD neuropathology, antemortem cognitive impairment, and disease duration; these correlations suggest that SIRT1 loss is associated with AD progression. Aging is central to AD pathogenesis, and growing evidence suggests that metabolic syndrome is linked to AD. Because SIRT1 activation may act against risk factors of AD by increasing longevity and regulating cellular metabolic processes, it is possible that the loss of SIRT1 we identified contributes to AD pathogenesis.

Among the brain regions investigated, greater losses of SIRT1 protein and mRNA were observed in the cerebral cortex, whereas no change was detected in the cerebellum. In the hippocampus, we found decreased SIRT1 transcripts in the CA1 and CA3 subregions, but not in the dentate gyrus. Interestingly, CA1 and CA3 subregions of the hippocampus are the target site of projecting neurons of the entorhinal cortex, which are among the first to develop neurofibrillary tangles in AD (52–54). In contrast, no such difference was detected by Western immunoblotting probably because the analysis was performed with homogenates from the whole hippocampal structure that precluded subregion analyses. Thus, overall, the reduction in SIRT1 was observed in AD-relevant regions but not in the cerebellum, a region that is relatively spared in AD. This pattern of loss suggests that a SIRT1 deficit occurs in affected brain regions over the course of AD progression.

It is not possible to determine exactly when SIRT1 loss occurs in AD, but our observations suggest that it is a relatively late event. First, we found a convincing relationship between SIRT1 and the duration of disease. This suggests that SIRT1 loss becomes more apparent in patients who have AD for a longer time; an observation inconsistent with an early occurrence. Second, individuals with MCI did not show any trend toward a decrease in SIRT1; statistically significant loss of SIRT1 occurred only in patients with the highest indices of AD neuropathology. That observation suggests that measurement of SIRT1 is unlikely to be of value as a marker in the early stages of AD. Third, no reduction of SIRT1 was detected in the 3×Tg-AD mouse model at ages when significant brain Aβ and tau pathologies are found. Because frank neuron loss is not observed in this transgenic mouse, it can be considered as a model of early AD, which does not progress to a stage at which SIRT1 loss would occur. Indeed, a reduction in SIRT1 expression was recently reported in the brains of senescence-accelerated mice (SAMP8 mice), supporting the contention that 3×Tg-AD mice may not model the aging characteristics necessary to reproduce the diminution of SIRT1 found in advance stages of AD (55). The present data are, therefore, consistent with the view that the decrease of SIRT1 occurs late in the disease, perhaps as a correlate of Aβ and tau pathologies.

Independent of its point of occurrence in the course of AD, a decrease of SIRT1 may have a wide range of consequences at the cellular level. A specific role of SIRT1 in the CNS has not been determined, but it is known to regulate a plethora of cellular cascades related to cell survival and metabolic homeostasis that likely affect brain cells (9–13, 23). Double labeling immunohistochemistry experiments in the mouse cortex using NeuN show that SIRT1 is mainly localized in neurons (24), whereas expression in astrocytes cannot be ruled out (56, 57). Transgenic mice that overexpress SIRT1 display improved glucose homeostasis and increased metabolic rates (15), 2 processes expected to be beneficial in AD (6). More specifically, a reduction of SIRT1 desacetylating action in AD brain could limit the capacity of AcetylCoA synthetase to generate AcetylCoA, a key molecule in cellular metabolism (58). Additional evidence from experiments in cultured neurons suggests that decreased SIRT1 activity could accelerate neurodegeneration through upregulation of nicotinamide mononucleotide adenylyltransferase 1 activity (59) or repression of p25-mediated cell death (60). In a more direct connection with Aβ production, SIRT1 loss might enhance the ROCK1-dependent γ-secretase cleavage of the amyloid precursor protein, thereby promoting the accumulation of Aβ (24). The present immunoblot data do not, however, support a modulation of ROCK1 levels in AD brains. In vitro evidence suggests that altered SIRT1 activity may also increase nuclear factor-κB signaling in microglia, which would exacerbate Aβ42 neurotoxicity (56). The significant correlation between SIRT1 and Aβ levels in the brain as seen in human patients (Table 3) and previously in squirrel monkeys (21) provides additional argument for a link between SIRT1 and Aβ production.

Brain samples in the present study were characterized for Aβ, tau, and synaptic abnormalities, making detailed correlative analyses possible. We found strong inverse relationships between the extent of tau pathology and the loss of SIRT1. This is particularly important because the conversion of normal tau into its detergent-insoluble PHF form usually correlates particularly well with cognitive impairment in AD (27, 32, 61–64). This association suggests that the conversion from normal tau into insoluble PHF shares common mechanistic pathways with the decrease in SIRT1 in AD, thus linking SIRT1 concentration to the severity of the disease. On the other hand, the relationships between SIRT1 and Aβ levels or between SIRT1 and synaptic markers were relatively weaker (except for p21-activated kinase). The stronger statistical significance between SIRT1 levels and Braak staging criteria, which focuses more on tangles compared with National Institute on Aging–Reagan or CERAD staging, also supports our correlative analyses. Therefore, these observations suggest the existence of a tight and specific link between the accumulation of tau and the regulation of SIRT1.

Mounting evidence suggests that brain fatty acids are involved in AD pathogenesis. The n-3 PUFA have received considerable attention because their concentrations in the

brain depend on dietary consumption. Epidemiological, postmortem, and animal studies provide arguments for n-3 PUFA to be considered as modifiable risk factors or as therapeutic targets in AD (37, 45–48). It has been speculated that n-3 PUFA could exert their action through regulation of SIRT1 activity (49). Our present data suggest that concentration in SIRT1 is indeed linked to DHA and EPA levels. Surprisingly, SIRT1 protein levels were positively and negatively linked to DHA and EPA, respectively. Brain EPA can be converted into DHA, which can be retroconverted into EPA, leading to an equilibrium where DHA concentrations are usually at least 20 times higher than EPA (65, 66). The present observation suggests that SIRT1 is involved in this state of equilibrium between EPA and DHA and apparently linked to the conversion of EPA into DHA. Despite the fact that we observed no correlation between SIRT1 and autopsy delays, we cannot rule out the possibility that postmortem biochemical events may have altered PUFA levels, thereby contributing in part to the relationships reported here.

It has been proposed that SIRT1 plays a critical role in aging processes, metabolism-related disorders, and possibly neurodegenerative diseases. Indeed, profound postmortem losses of SIRT1 were detected in the frontal cortex of patients with Huntington disease (55). Our present analyses have established a strong relationship between SIRT1 decrease, duration of AD symptoms, and the accumulation of tau. Altogether, these data indicate that the loss of SIRT1 accompanies AD neurodegeneration. Whether SIRT1 loss plays a causal role or is a consequence of other neuropathologic events is unknown, but the findings in Huntington disease indicate that SIRT1 loss can occur in the absence of tau pathology. Because a decrease in SIRT1 activity can clearly have deleterious effects on neuron health, therapeutic strategies aiming at increasing SIRTs activity in AD brain warrant further research.

ACKNOWLEDGMENTS

The authors thank Dr Frédéric Picard for constructive comments and Caroline Rancourt for technical support. The authors are indebted to all volunteers who participated in the Religious Orders Study and donors who contributed to the Douglas Hospital Research Centre Brain Bank.

REFERENCES

1. Goedert M, Spillantini MG. A century of Alzheimer's disease. Science 2006;314:777–81
2. Ferri CP, Prince M, Brayne C, et al. Global prevalence of dementia: A Delphi consensus study. Lancet 2005;366:2112–17
3. Mattson MP. Gene-diet interactions in brain aging and neurodegenerative disorders. Ann Intern Med 2003;139:441–44
4. Walsh DM, Selkoe DJ. Deciphering the molecular basis of memory failure in Alzheimer's disease. Neuron 2004;44:181–93
5. Irie F, Fitzpatrick AL, Lopez OL, et al. Enhanced risk for Alzheimer disease in persons with type 2 diabetes and APOE epsilon4: The Cardiovascular Health Study Cognition Study. Arch Neurol 2008;65: 89–93
6. Pasinetti GM, Zhao Z, Qin W, et al. Caloric intake and Alzheimer's disease. Experimental approaches and therapeutic implications. Interdiscip Top Gerontol 2007;35:159–75
7. Rönnemaa E, Zethelius B, Sundelöf J, et al. Impaired insulin secretion increases the risk of Alzheimer disease. Neurology 2008;71:1065–71
8. Whitmer RA, Gunderson EP, Quesenberry CP, et al. Body mass index in midlife and risk of Alzheimer disease and vascular dementia. Curr Alzheimer Res 2007;4:103–9
9. Anekonda TS, Reddy PH. Neuronal protection by sirtuins in Alzheimer's disease. J Neurochem 2006;96:305–13
10. Gan L, Mucke L. Paths of convergence: Sirtuins in aging and neurodegeneration. Neuron 2008;58:10–14
11. Nunomura A, Moreira PI, Lee HG, et al. Neuronal death and survival under oxidative stress in Alzheimer and Parkinson diseases. CNS Neurol Disord Drug Targets 2007;6:411–23
12. Dali-Youcef N, Lagouge M, Froelich S, et al. Sirtuins: The "magnificent seven," function, metabolism and longevity. Ann Med 2007;39:335–45
13. Guarente L, Picard F. Calorie restriction—the SIR2 connection. Cell 2005;120:473–82
14. Baur JA, Pearson KJ, Price NL, et al. Resveratrol improves health and survival of mice on a high-calorie diet. Nature 2006;444:337–42
15. Bordone L, Cohen D, Robinson A, et al. SIRT1 transgenic mice show phenotypes resembling calorie restriction. Aging Cell 2007;6:759–67
16. Cohen HY, Miller C, Bitterman KJ, et al. Calorie restriction promotes mammalian cell survival by inducing the SIRT1 deacetylase. Science 2004;305:390–92
17. Kaeberlein M, McVey M, Guarente L. The SIR2/3/4 complex and SIR2 alone promote longevity in *Saccharomyces cerevisiae* by two different mechanisms. Genes Dev 1999;13:2570–80
18. Picard F, Kurtev M, Chung N, et al. Sirt1 promotes fat mobilization in white adipocytes by repressing PPAR-gamma. Nature 2004;429:771–76
19. Halagappa VKM, Guo Z, Pearson M, et al. Intermittent fasting and caloric restriction ameliorate age-related behavioral deficits in the triple-transgenic mouse model of Alzheimer's disease. Neurobiol Dis 2007;26:212–20
20. Patel NV, Gordon MN, Connor KE, et al. Caloric restriction attenuates Abeta-deposition in Alzheimer transgenic models. Neurobiol Aging 2005;26:995–1000
21. Qin W, Chachich M, Lane M, et al. Calorie restriction attenuates Alzheimer's disease type brain amyloidosis in Squirrel monkeys (*Saimiri sciureus*). J Alzheimer's Dis 2006;10:417–22
22. Wang J, Ho L, Qin W, et al. Caloric restriction attenuates beta-amyloid neuropathology in a mouse model of Alzheimer's disease. FASEB J 2005;19:659–61
23. Outeiro TF, Marques O, Kazantsev A. Therapeutic role of sirtuins in neurodegenerative disease. Biochim Biophys Acta 2008;1782:363–69
24. Qin W, Yang T, Ho L, et al. Neuronal SIRT1 activation as a novel mechanism underlying the prevention of Alzheimer disease amyloid neuropathology by calorie restriction. J Biol Chem 2006;281: 21745–54
25. Julien C, Tremblay C, Bendjelloul F, et al. Decreased drebrin mRNA expression in Alzheimer disease: Correlation with tau pathology. J Neurosci Res 2008;86:2292–302
26. Mirra SS, Gearing M, McKeel DW, et al. Interlaboratory comparison of neuropathology assessments in Alzheimer's disease: A study of the Consortium to Establish a Registry for Alzheimer's Disease (CERAD). J Neuropathol Exp Neurol 1994;53:303–15
27. Tremblay C, Pilote M, Phivilay A, et al. Biochemical characterization of Abeta and tau pathologies in mild cognitive impairment and Alzheimer's disease. J Alzheimers Dis 2007;12:377–90
28. Bennett DA, Wilson RS, Schneider JA, et al. Natural history of mild cognitive impairment in older persons. Neurology 2002;59:198–205
29. Bennett DA. Postmortem indices linking risk factors to cognition: Results from the Religious Order Study and the Memory and Aging Project. Alzheimer Dis Assoc Disord 2006;20:S63–68
30. Bennett DA, Schneider JA, Bienias JL, et al. Mild cognitive impairment is related to Alzheimer disease pathology and cerebral infarctions. Neurology 2005;64:834–41
31. Wilson RS, Beckett LA, Barnes LL, et al. Individual differences in rates of change in cognitive abilities of older persons. Psychol Aging 2002; 17:179–93
32. Bennett DA, Schneider JA, Wilson RS, et al. Neurofibrillary tangles mediate the association of amyloid load with clinical Alzheimer disease and level of cognitive function. Arch Neurol 2004;61:378–84
33. Bennett DA, Wilson RS, Schneider JA, et al. Apolipoprotein E epsilon4 allele, AD pathology, and the clinical expression of Alzheimer's disease. Neurology 2003;60:246–52

34. Calon F, Morissette M, Rajput AH, et al. Changes of GABA receptors and dopamine turnover in the postmortem brains of parkinsonians with levodopa-induced motor complications. Mov Disord 2003;18:241–53
35. Kingsbury AE, Foster OJ, Nisbet AP, et al. Tissue pH as an indicator of mRNA preservation in human post-mortem brain. Brain Res Mol Brain Res 1995;28:311–18
36. Oddo S, Caccamo A, Shepherd JD, et al. Triple-transgenic model of Alzheimer's disease with plaques and tangles: Intracellular Abeta and synaptic dysfunction. Neuron 2003;39:409–21
37. Calon F, Lim GP, Yang F, et al. Docosahexaenoic acid protects from dendritic pathology in an Alzheimer's disease mouse model. Neuron 2004;43:633–45
38. Frye RA. Characterization of five human cDNAs with homology to the yeast SIR2 gene: Sir2-like proteins (sirtuins) metabolize NAD and may have protein ADP-ribosyltransferase activity. Biochem Biophys Res Commun 1999;260:273–79
39. Bousquet M, Saint-Pierre M, Julien C, et al. Beneficial effects of dietary omega-3 polyunsaturated fatty acid on toxin-induced neuronal degeneration in an animal model of Parkinson's disease. FASEB J 2008;22: 1213–25
40. Masood A, Stark KD, Salem N. A simplified and efficient method for the analysis of fatty acid methyl esters suitable for large clinical studies. J Lipid Res 2005;46:2299–305
41. Folch J, Lees M, Sloane Stanley GH. A simple method for the isolation and purification of total lipides from animal tissues. J Biol Chem 1957; 226:497–509
42. Sasaki T, Maier B, Bartke A, et al. Progressive loss of SIRT1 with cell cycle withdrawal. Aging Cell 2006;5:413–22
43. Terry RD, Masliah E, Salmon DP, et al. Physical basis of cognitive alterations in Alzheimer's disease: Synapse loss is the major correlate of cognitive impairment. Ann Neurol 1991;30:572–80
44. Zhao L, Ma QL, Calon F, et al. Role of p21-activated kinase pathway defects in the cognitive deficits of Alzheimer disease. Nat Neurosci 2006;9:234–42
45. Barberger-Gateau P, Raffaitin C, Letenneur L, et al. Dietary patterns and risk of dementia: The Three-City cohort study. Neurology 2007;69: 1921–30
46. Calon F, Cole G. Neuroprotective action of omega-3 polyunsaturated fatty acids against neurodegenerative diseases: Evidence from animal studies. Prostaglandins Leukot Essent Fatty Acids 2007;77:287–93
47. Morris MC, Evans DA, Bienias JL, et al. Consumption of fish and n-3 fatty acids and risk of incident Alzheimer disease. Arch Neurol 2003;60: 940–46
48. Schaefer EJ, Bongard V, Beiser AS, et al. Plasma phosphatidylcholine docosahexaenoic acid content and risk of dementia and Alzheimer disease: The Framingham Heart Study. Arch Neurol 2006;63:1545–50
49. Wu A, Ying Z, Gomez-Pinilla F. Omega-3 fatty acids supplementation restores mechanisms that maintain brain homeostasis in traumatic brain injury. J Neurotrauma 2007;24:1587–95
50. Kitazawa M, Oddo S, Yamasaki TR, et al. Lipopolysaccharide-induced inflammation exacerbates tau pathology by a cyclin-dependent kinase 5–mediated pathway in a transgenic model of Alzheimer's disease. J Neurosci 2005;25:8843–53
51. Oddo S, Caccamo A, Cheng D, et al. Genetically altering Abeta distribution from the brain to the vasculature ameliorates tau pathology. Brain Pathol 2008 (Jul 24; electronic publication ahead of print)
52. Gómez-Isla T, Price JL, McKeel DW, et al. Profound loss of layer II entorhinal cortex neurons occurs in very mild Alzheimer's disease. J Neurosci 1996;16:4491–500
53. Hyman BT, Van Hoesen GW, Damasio AR, et al. Alzheimer's disease: Cell-specific pathology isolates the hippocampal formation. Science 1984;225:1168–70
54. Hyman BT, Van Hoesen GW, Kromer LJ, et al. Perforant pathway changes and the memory impairment of Alzheimer's disease. Ann Neurol 1986;20:472–81
55. Pallàs M, Pizarro JG, Gutierrez-Cuesta J, et al. Modulation of SIRT1 expression in different neurodegenerative models and human pathologies. Neuroscience 2008;154:1388–97
56. Chen J, Zhou Y, Mueller-Steiner S, et al. SIRT1 protects against microglia-dependent amyloid-beta toxicity through inhibiting NF-kappaB signaling. J Biol Chem 2005;280:40364–74
57. Prozorovski T, Schulze-Topphoff U, Glumm R, et al. Sirt1 contributes critically to the redox-dependent fate of neural progenitors. Nat Cell Biol 2008;10:385–94
58. Hallows WC, Lee S, Denu JM. Sirtuins deacetylate and activate mammalian acetyl-CoA synthetases. Proc Natl Acad Sci U S A 2006; 103:10230–35
59. Araki T, Sasaki Y, Milbrandt J. Increased nuclear NAD biosynthesis and SIRT1 activation prevent axonal degeneration. Science 2004;305: 1010–13
60. Kim D, Nguyen MD, Dobbin MM, et al. SIRT1 deacetylase protects against neurodegeneration in models for Alzheimer's disease and amyotrophic lateral sclerosis. EMBO J 2007;26:3169–79
61. Arriagada PV, Growdon JH, Hedley-Whyte ET, et al. Neurofibrillary tangles but not senile plaques parallel duration and severity of Alzheimer's disease. Neurology 1992;42:631–39
62. Giannakopoulos P, Herrmann FR, Bussière T, et al. Tangle and neuron numbers, but not amyloid load, predict cognitive status in Alzheimer's disease. Neurology 2003;60:1495–500
63. Nagy Z, Esiri MM, Jobst KA, et al. Relative roles of plaques and tangles in the dementia of Alzheimer's disease: Correlations using three sets of neuropathological criteria. Dementia 1995;6:21–31
64. Näslund J, Haroutunian V, Mohs R, et al. Correlation between elevated levels of amyloid beta-peptide in the brain and cognitive decline. JAMA 2000;283:1571–77
65. Brossard N, Croset M, Pachiaudi C, et al. Retroconversion and metabolism of [13C]22:6n-3 in humans and rats after intake of a single dose of [13C]22:6n-3-triacylglycerols. Am J Clin Nutr 1996;64:577–86
66. Grønn M, Christensen E, Hagve TA, et al. Peroxisomal retroconversion of docosahexaenoic acid (22:6(n-3)) to eicosapentaenoic acid (20:5(n-3)) studied in isolated rat liver cells. Biochim Biophys Acta 1991;1081: 85–91

